Egypt. J. Chem. **Vol. 67**, No. 5 pp. 479 - 488 (2024)

Egyptian Journal of Chemistry

http://ejchem.journals.ekb.eg/

Analytical Techniques for Degradation Assessment of A Skeleton Dating Back to The Greco-Roman Period

Gomaa Abdel-Maksoud[a,*], Sawsan S. Darwish[1], Asmaa Hassaballah[b]

[a]*Conservation Department, Faculty of Archaeology, Cairo University, 12613 Giza*

[b]*Tanta Museum, Ministry of Tourism and Antiquities, Tanta, Egypt.*

Abstract

The Agricultural Museum in Giza, Egypt contains many archaeological bone artifacts. These include the studied skeleton. As a result of the inappropriate environmental conditions to which the skeleton was exposed both in the burial environment and in the museum's environment, there were many aspects of deterioration, including holes, different stains derived from various sources, accumulation of dust, dirt, color change, etc. This study aims to use analytical methods to diagnose the aspects of deterioration of a skeleton dating back to the Greco-Roman era and explain its deterioration mechanism to provide some recommendations regarding long-term conservation treatment that must be carried out in the next study. The authors prepared a new bone samples. Small fallen samples from the skeleton were used in the analytical study. Photographic and AutoCAD documentation were used to record the aspects of deterioration, Light microscope, scanning electron microscope (SEM), Attenuated Total Reflection – Fourier Transform Infrared Spectroscopy (ATR/FTIR), X-ray diffraction analysis (XRD), change of color, pH measurement, Isolation and identification of fungi were used to explain the deterioration mechanisms and estimate the conditions of the skeleton studied. The results of the photographic and AutoCAD documentation and light microscope showed some aspects of deterioration such as accumulated dust, discoloration, salt efflorescence, stains, erosion, missed parts, holes, etc. SEM investigation revealed the effect of environmental conditions on the surface morphology of the skeleton. FTIR analysis proved that some chemical changes occurred. pH value of different samples taken from the skeleton was in the level of acidity compared to modern bone, which was at the basic level.

Keywords: Baboon skeleton, Greco-Roman period, deterioration, documentation, analytical techniques.

1. Introduction

Many archaeological bone artifacts are found in museums, storage, and excavation. Chemically, bone consists of about 60--.70 wt% minerals, 20--.30 wt% collagen, and 10 wt% water [1]. The mineral content is primarily carbonated hydroxyapatite, with varying quantities of magnesium, sodium, fluorine, and strontium substituting for calcium, hydroxyl, or phosphate. Other elements, such as manganese, iron, and silicon, can exist as independent mineral phases within microscopic cracks and voids [2]. The organic phase of collagen consists of type I collagen, non-collagenous protein, liquids, mucopolysaccharides, and other components [3- 5].

The burial environmental conditions of archaeological bones play a significant role in preserving or deteriorating archaeological bones. Among the factors that affect archaeological bones in the burial environment and lead to their damage are soil type, pH value, water, salts, microorganisms, temperature, etc. Also, the exposure environment in museums is no less critical than the burial environment in damaging archaeological bones, especially exposure to fluctuations in temperature and relative humidity, exposure to access light, and the presence of air pollutants, in addition to the influence of microorganisms and insects. Accordingly, many aspects of deterioration appear on the archaeological bones, for example, stains derived from different sources, missing parts of the bones, pitting, turning, weakness and fragility, color change, etc [6- 9].

The sacred baboon was a recurring motif in ancient Egyptian art and religion, from Predynastic statuettes to later mortuary traditions, including reliefs, wall paintings, amulets, and statues—a tradition exceeding 3000 years. It was found in Egypt from the Predynastic period until the Greco-Roman period [10].

Some baboon skeletons in the Agricultural Museum in Giza, Egypt, are dated back to the Greco-

*Corresponding author e-mail: gomaa2014@cu.edu.eg

Receive Date: 28 September 2023,Revise Date: 04 November 2023, Accept Date: 09 November 2023

DOI: 10.21608/EJCHEM.2023.239495.8686

Roman era. They also suffer from some aspects of deterioration such as gaps, holes, cracks, dust, etc. as mentioned above.

It is vital to perform some highly efficient analyses and investigations to estimate the preservation conditions and interpret the deterioration mechanism to account for the deterioration process. Based on this, a long-term treatment plan can be drawn for the baboon skeleton.

Microscopic examination clearly shows aspects of deterioration on the surface of the bones, especially with scanning electron microscope. Attenuated Total Reflection – Fourier Transform Infrared Spectroscopy (ATR/FTIR) shows chemical changes in the functional groups of the chemical composition of the archaeological bones' organic and inorganic phases. X-ray diffraction is used to detect bone crystallinity. Color change using UV. A spectrophotometer is an essintial and accurate method for providing data that enables conservators to explain the mechanism of color change of bone. Measuring the pH value sometimes shows the effect of the burial or exposure environments on the archaeological bone and its reflection on the chemical changes. Microbiological examination is essential in detecting the type of microorganisms and their enzymatic activity, this enables restorers to determine the most appropriate sterilization materials to resist microbial damage [11- 18].

This study aims to conduct integrated analytical techniques (chemical, physical, and microbial) to determine the state of preservation of the studied skeleton, describe the aspects of its degradation, and explain its mechanics to draw up a long-term treatment plan that will be implemented in further research.

2. Materials and methods

2.1. Materials

2.1.1. New bone samples

Modern bone samples using sheep scapula were prepared according to some authors [3, 7, 8, 19]. Bone samples were boiled in distilled water. Then carefully clean the remnants of meat and fat with a blunt scalpel so as not to scratch the surface. Bone samples were dried at room temperature and modern samples were cut at 3.0 ×7.0 cm.

2.1.2. Archaeological samples

The sacred Baboon skeleton studied was found during the excavation of the Ashmounites area in Malawi, Minya Governance, Egypt. It dates back to the Greco-Roman period. It is now exhibited in the Agricultural Museum, Dokki, Giza, Egypt. Small samples were taken from those falling next to the skeleton for ATR/FTIR, XRD analysis, and measurement of pH value. The color change was measured directly in different places of the skeleton. The fungal examination was done using sterile swabs from various places in the studied structure.

2.2. Methods

2.2.1. Photographic documentation

The deterioration detected on the surface of the sacred Baboon skeleton was photographed with a digital camera (Samsung camera 38MP, f/2.2 lens slot) and described with the naked eye [20].

2.2.2. AutoCAD documentation

It is one of the most recent modern documentation methods used in the conservation field of archaeological objects. The photos taken from digital camera documentation have been elaborated using computer-aided design software (AutoCAD 2010) to show the dimensions and more details of the studied skeleton's deterioration [21].

2.2.3. Light microscope

Shenzhen Supereyesco makes the light microscope Model PZ01, LTD, China was used to investigate the surface of the studied skeleton. The magnification used was 50x.

2.2.4. Investigation of the surface morphology of the studied samples by Scanning Electron Microscope (SEM)

The change in the surface morphology of the studied samples was investigated using a Quanta 3D 200i made by FEI-accelerated voltage 20.00 kV. The observations were made on the examined samples without any preparation at low vacuum. A minute sample was taken from the fallen samples next to the studied skeleton.

2.2.5. Attenuated Total Reflection – Fourier Transform Infrared Spectroscopy (ATR/FTIR)

ATR-FTIR analysis was used to study the chemical changes in the functional groups present in the bone samples. For monitoring the existence and position of functional groups of the control and archaeological samples, The FTIR spectrum of each sample was taken from the upper part of the bone surface and was measured using a Bruker Vertex 70-platinum ATR spectrometer with crystal diamonds in the range of 4000–400 cm^{-1} and at a resolution 1 of 4 cm^{-1}.

2.2.6. X-ray diffraction analysis

The XRD measurements were done using the powder X-ray Diffraction (PanalyticalXPert Pro. Diffractometer) through (Cu Kα) radiation from 5 to 60 degrees. The Crystallinity index of modern and

archaeological samples was measured using x-ray diffraction (XRD) based on the full width of half maximum (FWHM) of the apatite diffraction 002 [22- 25].

2.2.7. Change of color

According to Abdel-Maksoud et al. [5] the change, of color for new and archaeological bone samples was measured using the CIE*Lab system. The 'L*' scale measures lightness. The 'a*' scale measures are red-green; +a means redder, and -a means greener. The 'b*' scale measures yellow-blue, and +b means more yellow, -b is bluer. Differences in color between two specimens are determined by the use of the Greek letter Delta (L, a & b). The total color difference (ΔE) is found according to the following equation:

$$\Delta E = \sqrt{(\Delta L)^2 + (\Delta a)^2 + (\Delta b)^2}$$

The measurement was made using Macbeth color eye 7000 (U.S.A.) UV spectrophotometer.

2.2.8. pH measurement

The pH of new and archaeological bone samples was measured. The samples were ground to powder according to the method of Abdel-Maksoud and Abdel-Hady [23] with some modifications. Mechanically, (0.25 g) from each bone sample was placed in 10 ml of deionized water (its pH was 7.4) for about six hours to allow the ions to transfer into the solution. The pH value was then measured using the ADWA waterproof pH tester of model AD11 at 22 °C ± 0.5 °C. The calibration of the pH was between 2 and 7. The pH value recorded in the results is the average of three readings for each sample. The standard deviation was ± 0.02.

2.2.9. Isolation and identification of fungi

To know the types of fungi growing samples, Czapek DOX agar medium was used, which consists of 30.0 gm Sucrose, 2.0 gm sodium nitrate $NaNO_3$, 1.0 gm dipotassium phosphate K_2HPO_4, 0.5 gm aqueous magnesium sulfate $MgSO_4.7H_2O$, 0.5gm potassium chloride KCl, 0.01 gm aqueous iron sulfate FeSO4.7H2O, 15.0 gm agar and 1000 ml distilled water, final pH 7.3 ± 0.2. The fungi growing on this medium were purified by using the single spore technique [26]. The obtained isolates were identified using the microscopic and cultural characteristics according to Gilman [27], Nelson [28], and Barnett and Hunter [29].

3. Results and discussion

3.1. Photographic documentation

The results (Fig. 1a & b) show the general view of the skeleton from the right and left sides. Fig. 1c shows the skeleton's skull from all directions (the cavity of eyes, nose, teeth, and fangs). Fig. 1d shows the rib cage from the right and left sides. Fig. 1e shows the presence of shoulder bones, tail, and spine extension is also observed.

It was clear from photographic documentation that the following aspects of deterioration were noticed:

Accumulated dust: Dust is considered one of the exhibited or stored collections in museums. In the current case of the studied skeleton, the source of dust may be from the burial environment of the skeleton or particulates from surrounding environmental conditions. The problem with this dust is that it promotes the growth of insects and microorganisms; it can contain some elements such as copper or iron which assist the conversion of some gaseous to acids such as the conversion of sulphur dioxide into sulphuric acid. It also leads to the deformation of the bone surface and disappears its aesthetic value.

Discoloration: Bone surface discoloration was observed on the surface of the studied skeleton. This discoloration may be due to various causal factors, including the chemical composition of the soil, fungal activity, heating events, decomposition of the flesh, duration of exposure to sunlight and cultural events, such as burial and ornamentation [30].

***Salt efflorescence*:** Blooming and crystallization of salts are observed in separate places of the skeleton, particularly in the thoracic cage; this may be due to the remains under the influence of the salty burial environment or containing a high percentage of salts. These salts have eroded a thin layer of the bone surface and have distorted the aesthetic appearance of the skeleton. Abdel-Maksoud and Abdel-Hady [23] confirmed that the soluble and insoluble salts greatly affected archaeological bones especially near agricultural lands.

***Erosion*:** Many causes lead to bone erosion, including but not limited to the effect of insects and microorganisms that secrete acids and enzymes that lead to interaction with the organic and inorganic components in archaeological bones and, at the end of the reaction, give rise to the erosion that was seen in the case of the current study.

***Missed parts*:** Many missing parts were observed, and this may be mainly due to various factors in the burial environment such as the influence of water, salts, decrease in pH value, microorganisms, insects, etc.

***Stains*:** Many stains on the skeleton's surface may be due to microorganisms, insects, salts, or improper handling after the excavation process, during transportation, or in the museum.

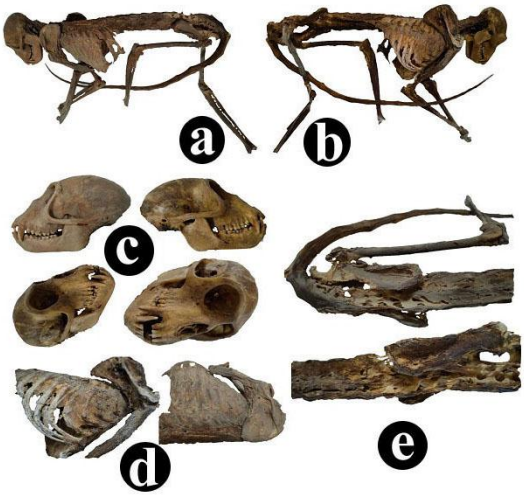

Fig. 1. Photographic documentation of the baboon skeleton: (a & b) The skeleton from the both sides; (c) Boboon skull from all directions, (d) baboon's rib cage on the right and left sides, (e) baboon's tail.

3.2. AutoCAD Documentation

It was clear from the results obtained (Fig. 2) using AutoCAD documentation that the total length of the baboon skeleton was 47 cm, and the full width was 18 cm. The same aspects of deterioration mentioned above are also inscribed on the drawing. To be more clear and more readable than the photographs.

3.3. Light microscope

The data obtained showed that the surface of the new bone sample (Fig. 3a) was smooth. Bone canals appear through tiny white or black dots. The bone surface is free of any aspects of deterioration. The results (Fig. 3b) showed the peeling of the outer layer of cement, with erosion in various places throughout the tooth. Color heterogeneity was also noted, and this was due to the contact of parts of the tooth with the burial environment. The deterioration is due to the possible decrease in the pH value or the presence of water-soluble salts with excessive water content in the burial soil. Fig. 3c shows some aspects of deterioration in a part of the bone (from the neck bottom of the skull). Micro-cracks, surface unevenness, color heterogeneity, color darkness, peeling of thin layers of the surface of the skull bone, and adhesion of accumulation dust have appeared. Fig. 3d-3f shows some aspects of deterioration to the floating ribs, such as uneven surface, corrosion, erosion, loss of some parts of them, and color change. Peeling off part of the bone surface was also noticed. Fig. 3g shows part of the spine of the studied skeleton with accumulated of dust, and color heterogeneity was also observed. Fig. 3h illustrates part of the bones of the feet. It was observed that part of the soil grains overlapped on the bone, which may be due to the increased porosity of the bone. Fig.3i shows part of a baboon's tail. It was evident that there was a color change and some corrosion.

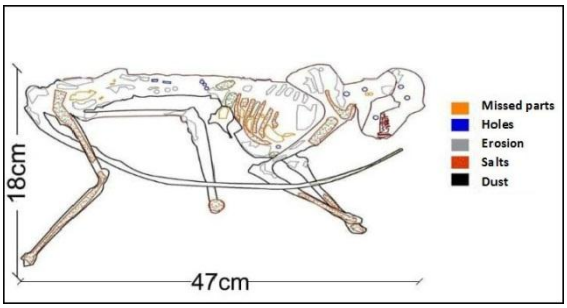

Fig. 2. AutoCAD Documentation for the size and aspects of seterioration of the studied skeleton.

3.4. Investigation of the surface morphology by a scanning electron microscope

Investigation with a scanning electron microscope showed severe deterioration to the surface morphology of the samples taken. The results show that the modern bone sample (Fig. 4a) has a flat and smooth surface. It shows bone channels, and there are no aspects of deterioration on the bone surface. The sample taken from the backbone (spine) of the skeleton (Fig. 4b) showed the destruction of the surface and giant cracks. It was also noted that the bone surface was not characterized by its distinct channels. The results taken from the lime-stained ribs (Fig. 4c) also showed surface distortion, the absence of a smooth surface of the bone, and the presence of lime bloom on the surface. There is some corrosion in various parts of the sample. A sample of dried meat taken from the neck (Fig. 4d) showed that this layer had been destroyed and eroded in some places, with the accumulation of dust and lime in other places.

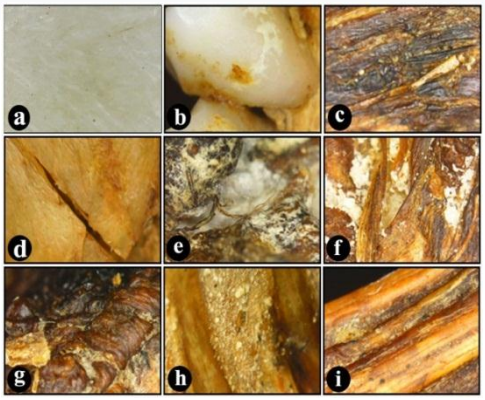

Fig. 3. Digital light microscope photos show some aspects of deterioration on different parts of the studied skeleton: (a) Modern sample; (b) tooth; (c) from the neck bottom of the skull; (d-f) Some parts of floating ribs; (g) Spine of the skeleton; (h) feet; (i) The nail.

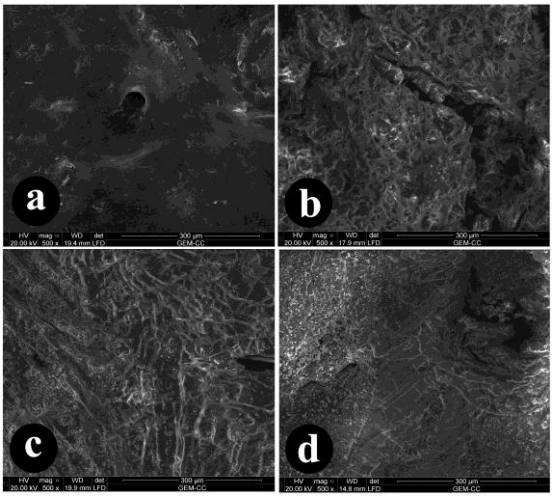

Fig. 4. Investigation of the surface morphology of different samples of the studied skeleton by SEM: (a) Modern bone sample; (b) sample from the backbone (spine); (c) Sample from the lime-stained rib; (d) Sample from the Dry flesh from the neck.

3.5. Attenuated Total Reflection – Fourier Transform Infrared Spectroscopy (ATR/FTIR)

ATR/FTIR analysis is important to identify the chemical changes in the organic and inorganic phases of the studied bone samples. The obtained results are explained as follows:

Organic phase

The results (Fig. 5) For organic phase showed that the band of amide A appeared at 3286.2 cm^{-1}, 3280.8 cm^{-1}, 3287.7cm^{-1}, 3281.7 cm^{-1} and 3264.6 cm^{-1} and their intensities were 0.019, 0.029, 0.039, 0.023 and 0.039 for the control (modern bone sample), lime-stained bone sample taken from rib, a sample of dry meat taken from the neck, and bone sample with part of burial soil respectively. This band referred to the strong and broadband corresponding to the stretching of both OH and NH groups diversely hydrogen-bonded [31- 34].

It was noticed that the wavenumbers of all archaeological samples and bone with soil shifted to lower values, but their intensities were increased compared to the control sample. On the contrary the lime-stained bone sample taken from the rib had the same wavenumber as the control sample, but its intensity increased. Amide B band appeared at 3071.2 cm^{-1}, 3074.6 cm^{-1}, 3066.7 cm^{-1} and 3050.8 cm^{-1} and their intensities were 0.012, 0.019, 0.026 and 0.016 for the control, and all archaeological samples mentioned above respectively, but this band disappeared with bone sample adhered with part of burial soil. This band is attributed to the Fermi resonance overtone of the amide II vibration [35]. The wavenumber of the lime-stained bone sample taken from the rib and the sample of dry meat taken from the neck decreased compared to the control sample, but the wavenumber of the archaeological bone with soil sample increased compared to the control sample. All archaeological samples increased in their intensities compared to the control sample. Amide I band appeared at 1630.4 cm-1, 1634.7 cm-1, 1627.6cm-1, 1633.4cm-1 and 1649.0cm-1, and their intensities were 0.042, 0.071, 0.087, 0.059 and 0.111 for the control, and all archaeological bone samples respectively. This band referred to the stretching vibrations of the peptide carbonyl group (C=O) coupled weakly with C-N stretching and N-H bending. It is sensitive to local order, and its exact position is determined by the backbone conformation and the hydrogen bonding pattern within the protein molecule [36].

Amide II band of the control, and all archaeological bone samples respectively appeared at 1539.2 cm^{-1}, 1537.4 cm^{-1}, 1537.9 cm^{-1} and 1540.9 cm^{-1} and their intensities were 0.044, 0.067, 0.058 and 0.099. This band disappeared with the lime-stained bone sample taken from the rib. This band is mainly derived from the C-N stretch along with N-H in-plane bending [37]. The wavenumber of a sample of dry meat taken from the neck decreased compared to the control sample, but for bone sample with part of burial soil increased. All samples were increased in their intensities compared to the control sample.

Amide III appeared at 1277.4 cm^{-1}, 1228.9 cm^{-1}, 1236.7 cm^{-1}, 1228.9 cm^{-1} and 1228.3 cm^{-1} and their intensities were 0.023, 0.058, 0.074, 0.048 and 0.104 for of the control, and all archaeological samples respectively. This band is referred to NH bending, CN stretching vibration and small contributions from CO in-plane bending and CC stretching vibration [35]. It was noticed that all wavenumbers were decreased with high intensities compared to the control sample.

By displaying the functional groups of the organic phase, the degradation of Collagen, the leading organic phase of bone, occurs via denaturation, hydrolysis, or oxidation. The denatured Collagen helix to disordered form gelatine has been characterized using infrared spectrophotometry in the amide II band shifts to lower wavenumber [38-40]. The amide II band for the control appeared at 1539.2 cm^{-1}. This band slightly decreased for all archaeological bone samples where it appeared respectively at 1539.2 cm^{-1}, 1533 cm^{-1}, 1537.4 cm^{-1}, and 1537.9 $cm^{-1,}$ except for the bone sample adhered with soil at 1540.9 cm^{-1}, this band is mainly derived from the C-N stretch and N-H in-plane bending [37].

Hydrolysis of the polypeptide chain caused an increase in the absorption intensity of OH stretching (amide A) or bending (amide I). By comparing the relative absorption intensities of the amide I band to that of the amide II, we found that the two bands are

nearly the same intensity in the spectrum for the control sample, while in the spectrum of archaeological samples, the amide I band is higher than the amide II [41].

Oxidation of the polypeptide chain results in the formation of carbonyl compounds, which can be seen as a slight shoulder on the amide I carbonyl band and may increase the area of the amide I band [41]; this can be observed in the archaeological sample from the backbone and the lime-stained bone sample from the ribs.

Inorganic phase

The spectral regions attributed to the CO_3^{2-} (type A) stretching band for of the control, a sample of dry meat taken from the neck, and a bone sample with part of burial soil, respectively appeared at 1451.9 cm^{-1}, 1434.0 cm^{-1}, 1454.2cm^{-1} and 1466.4 cm^{-1} and their intensities were 0.031 , 0.055 , 0.045 and 0.108. This band disappeared for lime-stained bone samples taken from the rib, The spectral regions attributed to the $COO\text{-}CO_3$ (carbonate: type B) for the same samples mentioned above appeared at 1400.8 cm^{-1}, 1412.8 cm^{-1}, 1415.8 $cm^{-1,}$ 1412.0 cm^{-1} and 1412.7 cm^{-1} and their intensities were 0.028, 0.062, 0.152, 0.050 and 0.133. It was noticed that all wavenumbers were increased with high intensities compared to the control sample. The spectral regions attributed to the O–C–O bending band, which referred to carbonate for the same samples mentioned above respectively appeared at 870.0 cm^{-1}, 875.2 cm^{-1}, 874.6 cm^{-1}, 874.2 cm^{-1} and 874.5 cm^{-1} and their intensities were 0.024, 0.043, 0.115, 0.035 and 0.109 . It was noticed that all wavenumbers were increased with high intensities compared to the control sample.

It was clear from the bands of carbonate, most of the wavenumbers shifted to high values for all archaeological bone samples with high intensities compared to the control sample. The strongest bands assigned to (PO_4^{-3}) symmetric stretch, which are mainly from hydroxyapatite appeared at 1025.8 cm-1, 1044.7 cm-1 and 1029.8 cm-1 with intensities 0.039, 0.052 and 0.106 for the control, the lime-stained bone sample taken from the rib, archaeological baboon bone, archaeological baboon bone + lime respectively. It was noticed that all wavenumbers were increased with high intensities compared to the control sample.

This band disappeared for a sample of dry meat taken from the neck, and bone sample with part of burial soil because it does not contain apatite. The other band assigned to ($PO4^{-3}$) (antisymmetric phosphate) for the same samples mentioned above appeared at 599.9 cm^{-1} and 571.7 cm^{-1}, and their intensities were 0.057 and 0.149 for the control and lime-stained bone sample taken from rib respectively. This band disappeared with a sample of dry meat taken from the neck, and bone sample with part of burial soil.

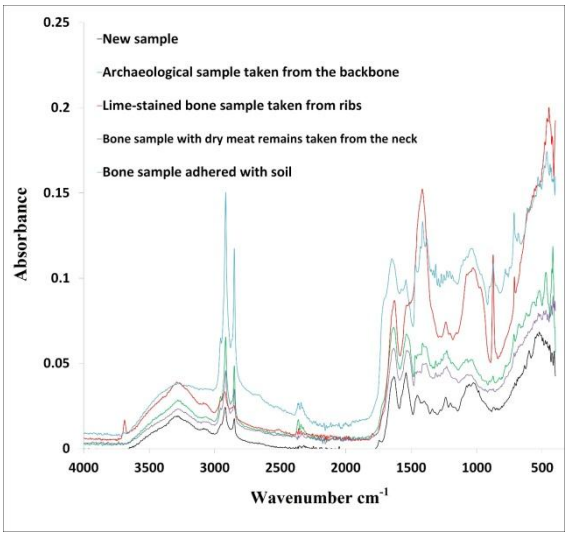

Fig. 5. ATR-FTIR analysis of new and archaeological samples

3.6. X-ray diffraction analysis

The main aim of X-ray diffraction analysis (Fig. 6) is to measure the crystallinity index of the studied bone samples. In this technique, the crystallinity index measurement by the width at half maximum of the 002 reflection was used according to Abdel-Maksoud [12]. The results proved that the crystallinity index of the modern sample was 0.90, but for the archaeological sample was 0.50, which indicated that it was more crystalline compared to the new bone sample. Abdel-Maksoud [12] said that bone mineral is generally described as having poor "crystallinity". He also reported that the increase in archaeological sample crystallinity may have been due to the loss of water, partially or totally decomposing the organic matter, or both of them.

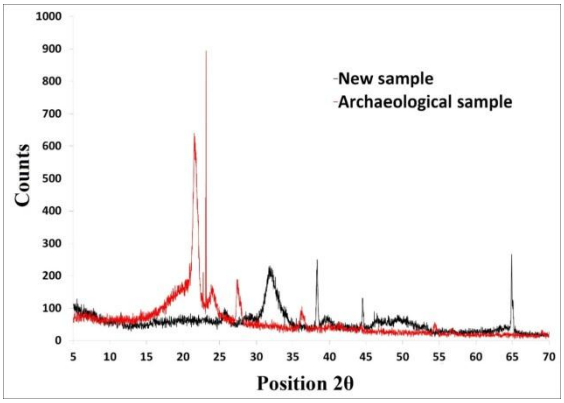

Fig. 6. X-ray diffraction analysis of new and archaeological bone samples.

3.7. Change of color

Measuring color change is an important measurement, as it gives a clear indication of the extent to which burial or exposure environments affect the state of bone preservation. The results of color change can be explained as follows:

The results (Fig. 7) showed that the lightness of the control sample was 81.32. The lightness in the archaeological samples decreased compared to the control sample. The reduction in L* value was 41%, 22%, and 41% for archaeological samples No. 1, 2, and 3 respectively. The red-green (a* value) results showed that the color of the control and archaeological samples No. 1 tended to be green color, but the color of the archaeological samples No. 2 and 3 tended to red. The yellow-blue (b* value) results that new and archaeological samples tended to be yellow in color. The highest yellow color was obtained from the archaeological sample No. 8. The total color difference (ΔE) indicated that there was a big change in the color of the archaeological sample. This proved that the different environments either in burial or in exhibitions in museums play a major role in these changes.

Dupras and Schultz [42] reported that normal fresh bone devoid of flesh has been described as having a yellowish-white to yellowish-brown color due to the retention of lipids and other fluids.

The discoloration of the bone surface may be due to a variety of causal factors, including the chemical composition of the soil, duration of exposure to sunlight, heating events, decomposition of the flesh, fungal activity, as well as cultural events, such as burial and ornamentation. Bradfield [30], and Krap et al. [43] reported that the changes in bone color are mainly caused by the thermal decomposition of type-1 collagen and the subsequent burning away of the residual carbon.

Table 1. Change of color of new and archaeological bone samples from different location of the baboon skeleton

Samples	Color values			Total color difference (ΔE)
	L*	a*	b*	
Control (new bone)	81.32	-2.79	9.50	0.0
Archaeological bone sample No. 1 (was taken from the tail).	47.91	-0.94	1.29	34.63
Archaeological bone sample No. 2 (bone stained with lime and was taken from the rib).	63.66	6.47	17.66	21.28
Archaeological bone sample No. 3 (was taken from the meat of the spine).	48.26	0.41	3.80	33.83

3.8. Measurement of pH:

It was clear from the data obtained (Table 2) that the pH of the control sample was 7.2, which indicates that it is at the alkaline level. This value is considered good and normal for bones in normal conditions. The pH of the soil sample was 6.2, and archaeological samples ranged from 5.9 to 6.1. This indicated the pH of the soil and archaeological samples in the acidity level.

Dorozhkin [44] explained the mechanism of the reaction of acid on calcium hydroxyapatite. He stated that when calcium hydroxyapatite reacts in an acidic solution containing many positive hydrogen ions, the apatite hydrolyzes (Equation 1).

This hydrolysis produces insoluble calcium phosphate and positive calcium ions and water are released (Equation 2).

Table 2. pH measurement of new and archaeological bone samples of the studied skeleton

Samples	pH value
Control (new bone).	7.2
Soil sample adhered with the skeleton.	6.2
archaeological bone (from the backbone).	6.1
archaeological bone (from lime-stained bone taken from rib).	6.0
Archaeological sample from dry meat taken from the neck.	5.9

The insoluble calcium phosphate compound also decomposes in the presence of more positive hydrogen ions (the reason for their presence is acid, as previously mentioned) into positive calcium ions and dissolved calcium phosphate (Equation 3). This is followed by the disintegration of calcium phosphate molecules dissolved in the acidic solution rich in positive hydrogen ions into more positive calcium ions and phosphoric acid (Equation 4).

$Ca_5(PO_4)_3(F\ OH) + H_2O + H+ = Ca_5(PO_4)_3(H_2O)^+ + HF\ H_2O$ (1)

$2Ca_5(PO_4)_3(H_2O)^+ = 3Ca_3(PO_4)_2 + Ca^{2+} + 2H_2O$ (2)

$Ca_3(PO_4)_2 + 2H^+ = Ca^{2+} + 2CaHPO_4$ (3)

$CaHPO_4 + H^+ = Ca^{2+} + H_2PO_4^-$ (4).

High et al. [45], and Ardhaoui et al. [46] also confirmed the disintegration of calcium phosphate mentioned above.

3.9. Identification of fungi

Seven species belonging to three genera were identified after their isolation from different areas of the skeleton studied. They were classified into: *Aspergillus flavus* (3 isolates from the skull, ribs and nail), *Aspergillus wentii* (1 isolate from the skull), *Aspergillus niger* (1 isolate from the ribs), *Aspergillus candidus* (1 isolate from the ribs), *Aspergillus fumigatus* (3 isolates from the pelvis, spine and tail), *Penicillium sp*. (2 isolates from the

ribs and tail), and *Alternaria alternata* (1 isolate from the pelvis) (Fig. 7).

The authors consider that identified fungi can be caused by the burial environment and the factors that encourage the growth of such fungi such as pH value, moisture, etc. They can also be the result of an uncontrolled environment in the museum'. The lack of control over the environmental conditions surrounding the studied skeleton has been found. Where there is frequency fluctuation between temperatures and relative humidity levels, no filters to absorb pollutants and particulates, etc.

Piepenbrink [47] reported that fungi are considered one of the most critical micro-organisms that play an essential role in the destruction of interred skeletal remains. He also said that Fungi are known to penetrate actively through hard tissues. Still, they also decompose dead bone by extensive excretion of secondary metabolites which partially leach the bone tissue. This leads to alterations in the quality and quantity of the organic and the inorganic bone matrix. Child [48] said that the bacteria and fungi able to produce collagenases at low temperatures are present in archaeological bone and associated soils. The bacteria and fungi are obligate aerobes, able to grow over a wide range of temperatures (4-39 0C) and pH values (3.6-9.0).

Hackett [49] stated that microorganisms from the burial environments cause the deterioration of bone through their penetration into the canal wall of buried bone and then attack the osteon tissue which results in Microscopical focal destruction (MFD).

Marchiafava [50] proved that the Infection of archaeological bones by fungi and bacteria may produce and cause MFD in buried human bone. Fungi and bacteria can demineralize bone resulting in histological destruction of bone otherwise known as “tunnels” or “borings”.

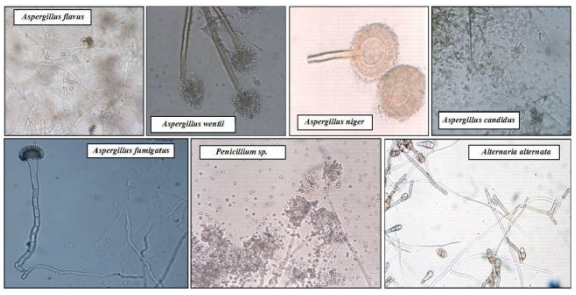

Fig. 7. Identified Fungi isolated from different areas of the studied skeleton.

4. Conclusion

The analytical techniques used in this study proved that the skeleton suffered from adverse deterioration. Digital camera, Digital light, and SEM microscopes showed many aspects of deterioration on the bone surface such as holes, missed parts, accumulated dust, erosion, absence of surface bone smoothness, etc. FTIR analysis proved that the chemical composition (organic and inorganic phases) was affected by the surrounding environmental conditions, and some changes occurred. X-ray diffraction analysis revealed that the crystallinity of archaeological bone was higher than that of modern bone. The UV spectrophotometer showed the change of color of archaeological samples compared to the control sample. The pH values of archaeological samples were found acidic. The dominant fungi isolated from different areas of the skeleton were *Aspergillus flavus*, *Aspergillus wentii*, *Aspergillus niger*, *Aspergillus candidus*, *Aspergillus fumigatus*, *Penicillium sp*., and *Alternaria alternate*. This study recommends conservation treatment, and preventive conservation processes for the studied skeleton in the next study.

Acknowledgement

The authors extend their sincere thanks, appreciation, and gratitude to the management staff of the Agricultural Museum in Giza, Egypt for providing all administrative assistance during the conduct of this research.

References

1. Reiche, I., Vignaud, C., and Menu. M., The Crystallinity of Ancient Bone and Dentine: New Insights By Transmission Electron Microscopy. Archaeom. Vol. 44, No. 3, 47–459 (2002).
2. North, A. E Biomimetic hydroxyapatite as a new consolidating agent for archaeological bone, Master of Arts in Archaeol. Anthropol. Sc., University of California, Los Angeles, 1-89 (2014).
3. Abdel-Maksoud, G., El-Sayed, A., Analysis of archaeological bones from different sites in Egypt by a multiple techniques (XRD, EDX, FTIR), Mediterr. Archaeol. Archaeom., Vol. 16, No 2, 149-158 (2016).
4. Abdel-Maksoud, G., El-Sayed, A., Microscopic investigation for condition assessment of archaeological bones from different sites in Egypt, Int. J. Conserv. Sci., Vol.7, No. 2, 381-394 (2016).
5. Abdel-Maksoud, G., Awad, H., Rashed, U. M., Elnagar, Kh., Preliminary study for the evaluation of a pulsed coaxial plasma gun for removal of iron rust stain from bone artifacts, J. Cult. Herit. Vol. 55, 128-137 (2022).
6. Abdel-Maksoud, G**.,** Marcinkowska, E., Effect of artificial heat ageing on the humidity sorption of of parchment and leathers compared with

archaeological samples, J. Soc. Leather Technol. Chem. Vol. 84, No. 5, 219-222 (2000).
7. Abdel-Maksoud, G., Kira, H. E., Mohamed, W. S., Consolidation of Fragile Archaeological Bone Artifacts: A review, Egypt. J. Chem. Vol. 65, No. SI:13, 1065 – 1080 (2022).
8. Abdel-Maksoud, A., Gaballah, S., Youssef, A. M., Eid, A. M., Sultan, M. H., Fouda, A., Eco-friendly approach for control of fungal deterioration of archaeological skeleton dated back to the Greco-Roman period, J. Cult. Herit. Vol. 59, 38-48 (2023).
9. Abdel-Maksoud, G., Ghozy, H., Ezzat, R., Helmy, M., Elsaka, M., Gamal, M., Mohamed, W. S., Evaluation of the efficiency of sodium alginate for the consolidation of archeological bones, Egypt. J. Chem. Vol. 66, No. 2, 357 – 366 (2023).
10. Dominy, N. J., Ikram, S., Moritz, G. L., Wheatley, P. V., Christensen, J. N., Chipman, J. W., Koch, P. L., Mummified baboons reveal the far reach of early Egypt. eLife, 9:e60860, 1-28 (2020).
11. Abdel-Maksoud, G., Evaluation of wax or oil/fungicide formulations for preservation of vegetable-tanned leather artifacts, J. Soc. Leather Technol. Chem. Vol. 90, No. 2, 58-67(2006).
12. Abdel-Maksoud G., Comparison between the properties of "accelerated-aged" bones and archaeological bones, Mediterr. Archaeol. Archaeom. Vol. 10, No. 1, 89-112 (2010).
13. Abdel-Maksoud, G., Elnagar, K., Ibrahim, M., Mohamed, O. A., Abdallah, A., Youssef, R., Elsayed, D., Labib, N., Mohamed, W. S., A comprehensive overview of the performance of polyamide 6 in the consolidation of vegetable-tanned leathers, J. Cult. Herit. Vol. 64, 207-215 (2023).
14. Abdel-Maksoud, G., Abdel-Nasser, M., Hassan, S. Eid, A. M., Abdel-Nasser, A., Fouda, A., Biosynthesis of titanium dioxide nanoparticles using probiotic bacterial strain, Lactobacillus rhamnosus, and evaluate of their biocompatibility and antifungal activity, Biomass Convers. Biorefin. 1-23(2023). https://doi.org/10.1007/s13399-023-04587-x
15. Abdel-Maksoud, G., Abdel-Nasser; M., Hassan, S., ; Eid, A. M., Abdel-Nasser, A., Fouda, A., Green synthesis of magnesium oxide nanoparticles using probiotic strain Lactobacillus gasseri and their activity against fungal strains isolated from historical manuscripts, Egypt. J. Chem. Vol. 66, No. 10, 179 – 189(2023).
16. Ismail, M., Abdel-Maksoud, G., The restoration of mummies in Ancient Egypt, Egypt. J. Chem. Vol. 66, No. 11, 163 – 175(2023).
17. Abdel-Nasser; M., Abdel-Maksoud, G., Eid, A. M., Hassan, S., Abdel-Nasser, A. Alharbi, M., Elkelish, A., Fouda, A., Antifungal activity of cell-free filtrate of probiotic bacteria *Lactobacillus rhamnosus* ATCC-7469 against fungal strains isolated from a historical manuscript, Microorganisms. 11, 1104, 1-23 (2023).
18. Abdel-Maksoud, G., Abdel-Hamied, M., Abdelhafez, A.A.M. Evaluation of the condition of a Mamluk-illuminated paper manuscript at Al-Azhar, Library Pigment. Resin Technol. Vol. 52/1, 49-59 (2023).
19. Gourrier, A., Bunk, O., Müller, K., Reiche, I., Artificially heated bone at low temperatures: a quantitative scanning-small-angle x-ray scattering imaging study of the mineral particle size, Archeo. Sciences, revue d'archéométrie, Vol. 35, pp. 191–199 (2011).
20. Abdel-Maksoud, G., Sobh, R. A., Tarek, A., Evaluation of MMI/acrylate nanocomposite with hydroxyapatite as a novel paste for gap filling of archaeological bones, J. Cult. Herit. Vol. 57, 194-204 (2022).
21. Abdel-Maksoud, G., Abdel-Hamied,, M., El-Shemy,H. A., Analytical techniques used for condition assessment of a late period mummy, J. Cult. Herit. Vol. 48, 83-92 (2021).
22. Hedges, R.E.M., Millard, A.R., Pike, A.W.G., Measurements and relationships of diagenetic alteration of bone from three archaeological sites. J. Archaeol. Sci. Vol. 22, No. 2, 201-209 (1995).
23. Abdel-Maksoud G, Abdel-Hady , M., Effect of burial environment on crocodile bones from Hawara excavation, Fayoum, Egypt. J. Cult. Herit. 12(2), 180-189 (2011). https://doi.org/10.1016/j.culher.2010.12.002 .
24. Zizak, I., Poschger, P., Paris, O., Misof, B.M., Berzlanovich, A., Bernstorff, S., Amenitsch, H., Klaushofer, K., Fratzl, P., Characteristics of mineral particles in the human bone, Cartilage interface, J. Struct. Biol., Vol. 141, 208-217 (2003).
25. Danilchenko, S.N., Moseke, C., Sukhodub, L.F., Sulkio.Cleff, B., X.ray diffraction studies of bone apatite under acid demineralization, Cryst. Res. Technol. Vol. 39, No. 1, 71 – 77(2004).
26. Manandhar, J.B., Hartman, G.L., Wang, T.C., Conidial germination and appressorial formation of Colletotrichum capsici and C. gloeosporioides isolates from Pepper, Plant Dis. 79, 361-366(1995).
27. Gilman, J.C A., Manual of Soil Fungi, (2nd ed.), The Iowa State University Press, Ames, Iowa, U.S.A (1957).
28. Nelson, P.E., Toussoun, T.A., Marasas, W.F.O., *Fusarium spp*., An Illustrated Manual for

Identification, The Pennsylvania University Press (1982).
29. Barnett, H. L., Hunter, B. B., Illustrated Genera of Imperfect Fungi. (4th ed.), Macmillan, New York (1986).
30. Bradfiel, J., Some thoughts on bone artefact discolouration at archaeological sites, J. Archaeol. Sci.: Reports, Vol. 17, pp. 500-509(2018).
31. Abdel-Maksoud, G., Al-Shazly, E.E.A., El-Amin,A., Damage caused by insects during mummification process: An experimental study, Archaeol. Anthropol. Sci. Vol. 3,No. 3, 291-308 (2011).
32. Saada, N. S., Abdel-Maksoud, G., Abd El-Aziz, M. S., Youssef, A. M., Evaluation and utilization of lemongrass oil nanoemulsion for disinfection of documentary heritage based on parchment, Biocatal. Agric. Biotechnol. Vol. 29. 101-839(2020).
33. Saada N, Abdel-Maksoud G, Abd El-Aziz M, Youssef A., Green synthesis of silver nanoparticles, characterization, and use for sustainable preservation of historical parchment against microbial biodegradation, Biocatal. Agric. Biotechnol. Vol. 32, 101948 (2021). (https://doi.org/10.1016/j.bcab.2021.101948
34. Abdel-Maksoud, G., Abdel-Nasser, M., Sultan, M. H., Eid, A. M., Alotaibi, S. H., Hassan, S. E., Fouda, A., Fungal Biodeterioration of a Historical Manuscript Dating Back to the 14th Century: An Insight into Various Fungal Strains and Their Enzymatic Activities. Life, Vol. 12, 1821,1-24(2022).
35. Vyskočilová, G., Carşote, C., ševčík, R., Badea, E., Burial.induced deterioration in leather: a FTIR.ATR, DSC, TG/DTG, MHT and SEM study, J. Herit. Science, Vol. 10:7,1-14 (2022).
36. Sebesty´en, Z., Badea, E., Carsote, C., Cz´eg´eny, Z., Szabó, Babinszki, B., Bozi, J., Jakab, A., Characterization of historical leather bookbindings by various thermal methods (TG/MS, Py-GC/MS, and micro-DSC) and FTIR-ATR spectroscopy, J. Anal Appl Pyrolysis. Vol. 162,: 105428, 1-12(2022).
37. Massadikova, G., Karadag, R., Pars, A., Ozomay, M., Physicochemical characterization of leather objects of the byzantine period, Mediterr. Archaeol. Archaeom. Vol. 20, No 3, 107-119 (2020).
38. Brodsky-Doyle, B.; Bendit, E.G.; Blout, E.R., "Infrared Spectroscopy of Collagen and Collagen-Like Polypeptides", *Biopolym.* 14, 937-957(1975).
39. Susi, H.; Ard, J.S.; Carroll, R.J.., "Hydration and Denaturation of Collagen as Observed by Infrared Spectroscopy", J. Am. Leather Chem. Assoc., 66 (11), 508-519(1971).
40. Warren, J.R.; Smith, W.E.; Tillman, W.J., "Internal Reflectance Spectroscopy and the Determination of the Degree of Denaturation of Insoluble Collagen", *J. Am. Leather* Chem. Assoc. 64 (1), 4-11(1969).
41. Derrick, Michele. "Evaluation of the State of Degradation of Dead Sea Scroll Samples Using FT-IR Spectroscopy." Book and Paper Group Annual 10: 49-651991.
42. Dupras, T. L., Schultz, J. J., Taphonomic Bone Staining and Color Changes in Forensic Contexts, chapter 12, In: Manual of Forensic Taphonomy, edited by Pokines, J. T., Symes, S. A. , 315-339(2013).
43. Krap, T., Ruijter, J. M., Nota, K., Karel, J., Burgers, A. L., Aalders, M. C. G., Oostra, R-J., Duijst, W., Colourimetric analysis of thermally altered human bone samples, Sci. Rep., 9:8923, 1-10 (2019).
44. Dorozhkin, S. V., Dissolution mechanism of calcium apatites in acids: A review of literature, World. j. Methodol. Vol. 2, No. 1, 1-17 (2012).
45. High, k., Milner, N., Panter, I., Penkman, K. E. H., Apatite for destruction: investigating bone degradation due to high acidity at Star Carr, J. Archaeol. Sci. Vol. 59, 159-168 (2015).
46. Ardhaoui, K., Bechrifa A. B., Jemal, M., Calcium hydroxyapatite solubilisation in the hydrochloric and perchloric acids, J. Therm. Anal. Calorim. Vol. 81, No. 2, 251-254 (2005).
47. Piepenbrink, H., Two Examples of Biogenous Dead Bone Decomposition and their Consequences for Taphonomic Interpretation, J. Archaeol. Sci. Vol. 13, 417-430 (1986).
48. Child, A. M., Microbial taphonomy of archaeological bone, Stud. Conserv. Vol. 40, 19-30 (1995).
49. Hackett, C.J., Microscopical focal destruction (tunnels) in exhumed human bones, Medic. Science and Law, Vol. 21, 243-265(1981).
50. Marchiafava, V., Bonucci, E. and Ascenzi, A., Fungal Osteoclasia: A model of dead bone resorption, Calc. Tiss. Res. Vol. 14, 195-210 (1974).